

1
2
3
4
5
6
7
8
9
10
11
12
13
14
15
16
17
18
19
20
21
22
23
24
25
26
27

Cyanobacterial Growth on Municipal Wastewater Requires Low Temperatures

Travis C. Korosh^{a,b}, Andrew Dutcher^c, Brian F. Pflieger^{a,d}, and Katherine D. McMahon^{c,e}*

^a Department of Chemical and Biological Engineering, University of Wisconsin-Madison, Madison, WI 53706, United States

^b Environmental Chemistry and Technology Program, University of Wisconsin-Madison, Madison, WI 53706, United States

^c Department of Civil and Environmental Engineering, University of Wisconsin-Madison, Madison, WI 53706, United States

^d Microbiology Doctoral Training Program, University of Wisconsin-Madison, Madison, WI 53706, United States

^e Department of Bacteriology, University of Wisconsin-Madison, Madison, WI 53706, United States

* Corresponding author. 5552 Microbial Science Building, 1550 Linden Drive, Madison, WI 53706, United States. Phone: +1 608 890 2836. Fax: +1 608 262-9865. E-mail address: trina.mcmahon@wisc.edu.

Keywords: Nutrient removal, cyanobacteria, Synechococcus strain PCC 7002

28 **ABSTRACT**

29 Side-streams in wastewater treatment plants can serve as concentrated sources of
30 nutrients (i.e. nitrogen and phosphorus) to support the growth of photosynthetic organisms that
31 ultimately serve as feedstock for production of fuels and chemicals. However, other chemical
32 characteristics of these streams may inhibit growth in unanticipated ways. Here, we evaluated the
33 use of liquid recovered from municipal anaerobic digesters via gravity belt filtration as a nutrient
34 source for growing the cyanobacterium *Synechococcus* sp. strain PCC 7002. The gravity belt
35 filtrate (GBF) contained high levels of complex dissolved organic matter (DOM), which seemed
36 to negatively influence cells. We investigated the impact of GBF on physiological parameters
37 such as growth rate, membrane integrity, membrane composition, photosystem composition, and
38 oxygen evolution from photosystem II. At 37°C, we observed an inverse correlation between
39 GBF concentration and membrane integrity. Radical production was also detected upon exposure
40 to GBF at 37°C. However, at 27°C the dose dependent relationship between GBF concentration
41 and lack of membrane integrity was abolished. Immediate resuspension of strains in high doses
42 of GBF showed markedly reduced oxygen evolution rates relative to the control. Together, this
43 suggests that one mechanism responsible for GBF toxicity to *Synechococcus* is the interruption
44 of photosynthetic electron flow and subsequent phenomena. We hypothesize this is likely due to
45 the presence of a phenolic compounds within the DOM.

46

47 INTRODUCTION

48 The need to develop non-petroleum based platforms for fuel and chemical production is
49 driving researchers to explore alternatives that harness renewable energy sources while
50 minimizing other environmental impacts such as freshwater depletion, eutrophication, and the
51 use of arable land for non-food production. Cyanobacteria are particularly attractive such
52 platforms due to their genetic tractability, rapid growth rates, halotolerance, and ability to be
53 grown on non-productive land with simple nutrient requirements (1, 2). According to published
54 life cycle assessments, a large portion of the associated costs of culturing photoautotrophs are
55 tied to upstream costs, such as CO₂ delivery and fertilizer application (3). High
56 phosphorous/nitrogen removal rates and energy efficiencies have been reported for
57 photobioreactor and open pond cultivation systems using wastewater streams rich in nitrogen and
58 phosphorus (4, 5). Therefore, it may be possible to offset the requirement for fertilizer by
59 reclaiming nutrients from wastewater. This approach could yield the sought-after non-petroleum
60 based alternative while also providing a more effective means of nutrient and metal removal than
61 conventional wastewater treatment (6–8). Side-streams from common wastewater treatment
62 facilities such as supernatants or filtrates from solids-separation processes are particularly
63 promising nutrient sources, assuming that cyanobacterial strains can efficiently use them.

64 Of the many streams available in common wastewater facilities, the liquid fraction of
65 anaerobic digestate is thought to be the most attractive nutrient source (8–11). Although digestate
66 is rich in the inorganic constituents necessary for growth, it also contains dissolved organic
67 matter (DOM) that has been shown to limit photosynthetic activity (12). DOM is a heterogenous
68 mixture of aliphatic and aromatic compounds derived from the decomposition of living
69 organisms (13). The chemical nature of wastewater-derived DOM is largely governed by the

70 type of treated waste and the treatment process, but it is largely comprised of hydrophilic, fulvic,
71 and humic substances (14, 15). Humics can induce damaging permeability in model and bacterial
72 membranes (16, 17). Various studies have also demonstrated that fulvic and humic acids can
73 enhance the solubility of many organic compounds (18), which in turn would augment their
74 bioavailability and potential toxicity. Many of these compounds are also photo-reactive,
75 producing toxic hydrogen peroxide and hydroxyl radicals (19, 20), which is of significant
76 concern for phototroph cultivation.

77 The mode of DOM toxicity is thought to involve interactions with the protein-pigment
78 complex of photosystem II (PSII) in photosynthetic organisms, although the exact molecular
79 mechanism remains unclear (21). When the rate of light induced damage to PSII exceeds its rate
80 of repair, growth suppression and chlorosis result from the phenomena known as photoinhibition
81 (22). When damage by photoinhibition is sufficient to hamper the natural ability to consume
82 electrons generated by photosynthesis, reactive oxygen species (ROS) are concomitantly
83 produced as an undesired by-product. Prolonged oxidative stress halts protein translation through
84 oxidation of specific cysteine residues in the ribosomal elongation factors (23). Given these
85 findings, it is increasingly evident that under conditions of sustained stress, regulation of electron
86 flow is critical to maintain homeostasis in photosynthetic organisms (24, 25). Thus, it is
87 important to understand the mechanisms by which DOM may be interrupting electron flow in
88 order to capitalize on the potential of cyanobacteria to remediate wastewater and generate high-
89 value chemicals.

90 In this study, we tested the practicality of using combined streams from a municipal
91 wastewater plant as a nutrient source for cyanobacterial cultivation. We used the euryhaline
92 cyanobacteria *Synechococcus* sp. strain PCC 7002 (PCC 7002) due to its exceptional tolerance to

93 high-light intensity, salt, and other environmental stresses (26, 27). Initial attempts to grow PCC
94 7002 in this nutrient source under standard environmental conditions of 1% (v/v) CO₂, a
95 temperature of 37°C, and illumination of 200 μmol photons m⁻²s⁻¹ resulted in photobleached
96 (white-yellow) cultures. In an effort to explain this observation while developing more feasible
97 cultivation conditions, we assessed the effects of many environmental parameters during PCC
98 7002 cultivation in wastewater-based media by monitoring changes in growth rate, photopigment
99 abundance, oxygen evolution rates, membrane integrity, and membrane composition. We
100 observed a concentration and temperature dependent effect of GBF towards membrane and
101 photosystem degradation. High GBF concentrations were associated with elevated DOM levels,
102 and produced ROS in 37°C grown cultures. At 27°C, cultures adapted to growth on GBF had
103 elevated levels of total fatty acids, high unsaturated fatty acid content, and elevated membrane
104 integrity. Decreased photosynthetic oxygen production rates were noted upon exposure to high
105 levels of GBF. This suggests bioavailability of the photoinhibitory compound in GBF is
106 governed by changes in membrane content and composition that occur during growth at
107 relatively high temperatures.

108

109 **MATERIALS AND METHODS**

110 *Media and Growth Conditions*

111 *Synechococcus* sp. strain PCC 7002 was obtained from the Pasteur Culture Collection of
112 Cyanobacteria. Experiments were performed with a strain of PCC 7002 harboring a gentamicin
113 resistance marker in the A2842 locus to maintain axenic cultures. Strains were grown and
114 maintained on Medium A⁺ (28) with 1.5% Bacto-Agar with gentamicin (30 μg/mL). Strains were

115 cultured in 250 ml baffled flasks with 50 mL Medium A⁺ with 5 μM NiSO₄ (29) with 1% CO₂-
116 enriched air at 150 rpm in a Kuhner ISF1-X orbital shaker. Temperature was maintained at 37°C
117 or 27°C and light intensity was fixed at approximately 200 μmol photons m⁻²s⁻¹ or 100 μmol
118 photons m⁻²s⁻¹ via a custom LED panel. Strains were pre-acclimated to the culture conditions
119 overnight before inoculating in fresh media. Optical density at 730 nm was measured in a Tecan
120 M1000 plate reader.

121 Wastewater-derived media was obtained from the Nine Springs Wastewater Treatment
122 Plant (Dane County, Wisconsin, USA). The plant is configured for biological nutrient removal
123 via a modified University of Cape Town process with no internal nitrate recycling and stable
124 performance yielding high secondary effluent quality (total phosphorus < 1 mg P/L, ammonia <
125 1 mg N/L, nitrate ~ 15 mg N/L) (30). Anaerobic digesters are used for solids stabilization and the
126 resulting digested material is passed over a gravity belt filter for dewatering. The system includes
127 an Ostara WASSTRIP process to recover phosphorus. This filtrate (GBF) served as the primary
128 source of phosphorus and reduced nitrogen for our cultures, and effluent from the post-
129 mainstream secondary treatment clarifier (secondary effluent) served as a diluent. GBF was
130 filtered through a paper filter to remove any exceptionally large flocs, then stored at -80°C until
131 use. Secondary effluent was collected one to four days before each experiment and held under
132 refrigeration at approximately 2°C. Experimental media was comprised primarily of secondary
133 clarifier effluent and GBF, combined in different proportions. Unless otherwise noted, GBF was
134 used at a concentration of 12.5% (v/v) in secondary effluent. To meet complete nutrient
135 requirements, the diluted GBF media was supplemented with trace metals and vitamin B12 at the
136 concentrations found in Medium A⁺, as well as KH₂PO₄ at a molar ratio of 1:32 soluble reactive
137 phosphorus (SRP) to bioavailable nitrogen (the sum of NH₄⁺ and NO₃⁻). All media was buffered

138 with Tris-HCl and adjusted to pH 8.0 with potassium hydroxide or hydrochloric acid before
139 sterilization by autoclaving.

140 *Staining, Flow Cytometry, and Fluorescence Measurements*

141 The membrane integrity of cyanobacteria cells was recorded by a flow cytometer
142 (FACSCalibur, BD Biosciences, San Jose, CA, USA). After growth in the respective media, cells
143 were centrifuged (2 minutes, 5000 RCF), decanted, and resuspended in 1 mL of Tris-Buffered
144 Saline (TBS) solution (pH 8.0). To identify membrane-compromised cells, SYTOX Green (Life
145 Technologies) was also added to each sample (1 μM). SYTO 59 (Life Technologies) was added
146 to each sample (1 μM) as a nucleic acid counterstain. As a control for a permeabilized
147 membrane, cells were resuspended in 190 proof ethanol. SYTOX green fluorescence was
148 visualized using 488 nm laser excitation and emission area was read using a 530/30 nm bandpass
149 filter. The 633 nm laser coupled with a 661/16 bandpass filter was used for SYTO 59
150 visualization. Analysis of the cytometric data was carried out with CellQuest Pro
151 (BDBiosciences, San Jose, CA, USA) software.

152 To assess reactive oxygen species production, cells ($\text{OD}_{730} = 1$) were incubated overnight
153 in Medium A, GBF, GBF + 1 mM Dithiothreitol (DTT), GBF + 1 mM N-acetylcysteine (NAC),
154 or Medium A + 100 μM methyl viologen as a positive control at 37°C with 5% CO_2 at a light
155 intensity of 200 $\mu\text{mol photons m}^{-2}\text{s}^{-1}$. Cells were washed in TBS, and either Sytox Green (1 μM)
156 or CellROX Orange reagent (Life Technologies) (5 μM) was added. After 30 min incubation in
157 darkness at 37°C, fluorescence was measured (Ex/Em 545/565 nm for Cell ROX Orange) and
158 (Ex/Em 504/523 nm for Sytox Green) in a Tecan M1000 plate reader.

159 *GBF Characterization*

160 SRP, ammonia, nitrate, and nitrite concentrations were determined for all secondary
161 clarifier effluent and GBF samples used in these experiments. In addition, the GBF was tested
162 for total suspended solids (TSS), volatile suspended solids (VSS) total solids (TS), and chemical
163 oxygen demand (COD). Ammonia, SRP, and COD were determined by colorimetric tests using
164 reagents from Hach. Nitrate and nitrite were determined using high performance liquid
165 chromatography (Shimadzu) with a C18 column and photodiode array detector (31). TSS, VSS,
166 and TS were measured according to Standard Method 2540 D, 2540 E, and 2540 B, respectively,
167 with 47mm diameter glass fiber filters (Whatman) used for TSS and VSS (32). Fluorescence
168 EEM measurements were conducted using a M1000 Tecan plate reader using a UV-transparent
169 plate (Costar 3635). Fluorescence intensity was normalized to quinine sulfate units (QSU), where
170 1 QSU is the maximum fluorescence intensity of 1 ppm of quinine sulfate in 0.1 N H₂SO₄ at
171 Ex/Em = 350/450. Rayleigh scatter effects were removed from the data set.

172 *Biochemical analyses*

173 Batch cultures were further assayed for dry cell weight (DCW), fatty acid content,
174 oxygen evolution rates, and chlorophyll a content. Cells were concentrated by centrifugation,
175 washed in TBS, and lyophilized overnight to obtain dry cell weights (DCW). Fatty acids from
176 approximately 10 mg of DCW with 10 mg ml⁻¹ pentadecanoic acid as an internal standard were
177 converted to methyl-esters, extracted with n-hexane and analyzed by GC-FID on a Restek
178 Stabilwax column (60m, 0.53 mm ID, 0.50 μm) (33). Photosynthetic oxygen evolution from
179 whole cells was measured with a Unisense MicroOptode oxygen electrode with 10 mM NaHCO₃
180 illuminated with a slide projector at PPFD from 76-2700 μmol m⁻² s⁻¹ for 30 min at room
181 temperature (34). Cells were collected by centrifugation and resuspended in the appropriate
182 media to give an OD₇₃₀ = 1.0. Chlorophyll a measurements were done via a 100% chilled

183 methanol extraction procedure (35). Chlorophyll a was calculated via the following equation:
184 $\text{Chl}_a = 16.29 * A^{665} - 8.54 * A^{652}$ (36).

185

186 **RESULTS**

187 *GBF and secondary effluent characteristics*

188 We measured nutrient concentrations from the batches of GBF collected over the 6
189 month experimental period (Table 1 and Table 2), to ascertain if it was a stable and reliable
190 nutrient source for cultivating the cyanobacteria. Sampling points from the Nine Springs
191 Wastewater Treatment Plant (Dane County, Wisconsin, USA) are shown in Figure 1. In order to
192 calculate nutrient stoichiometries, we took the sum of $\text{NH}_3\text{-N}$ and $\text{NO}_3\text{-N}$ to be the bioavailable
193 N. Nutrient levels in the GBF were markedly more variable than in the secondary effluent. The
194 average molar ratio of bioavailable N to SRP was 35 ± 7 in GBF diluted with secondary effluent
195 (12.5% v/v), as compared to 32 in Medium A⁺.

196 We also measured DOM quality in the secondary effluent and GBF using
197 excitation–emission matrix (EEM) fluorescence spectroscopy (37) because we hypothesized that
198 DOM was linked to toxicity during cultivation. Secondary effluent contained diffuse
199 constituents, including humic [excitation wavelengths (>280 nm) and emission wavelengths
200 (>380 nm)] and fulvic acid-like [excitation wavelengths (<250 nm) and emission wavelengths
201 (>350 nm)] spectra relative to Medium A⁺ (Figure 2). The distinction between the two substances
202 is historically based on solubility (38), but compositionally, fulvic acids contain more acidic
203 functional groups than humic acids (39). The fulvic acid content in media preparations rose with
204 increasing concentrations of GBF. Additionally, at high concentrations of GBF, a distinct region
205 [excitation wavelengths (270 -290 nm) and emission wavelengths (340-400 nm)] was attributed

206 to the presence of soluble microbial products, which include aromatic amino acids,
207 carbohydrates, or phenols (37, 40). The exact composition of these products varies with plant
208 configuration, but they are refractory to microbial degradation (41).

209 *Exposure to GBF at high temperatures generates radicals*

210 Preliminary growth experiments using GBF as a nutrient source were unsuccessful under
211 standard cultivation conditions, due to cell photobleaching. We hypothesized that DOM in the
212 media was in some way compromising membrane integrity, possibly via intracellular production
213 of reactive oxygen species (ROS). Thus, we measured the ROS content and loss of membrane
214 integrity in response to overnight GBF exposure at 37°C (Figure 3). We also examined the
215 capacity of reducing agents Dithiothreitol (DTT) or N-acetylcysteine (NAC) to quench the media
216 toxicity, since they have anti-oxidant properties due to the direct reduction of disulfide bonds or
217 as precursors for the anti-oxidant glutathione (42). To measure their effect on the ROS
218 production and culture viability after GBF exposure, we assessed ROS content and membrane
219 integrity with either concurrent addition or preincubation of these quenching compounds in the
220 diluted (12.5% v/v) GBF media. Addition of 100 µM methyl viologen to Medium A⁺ served as a
221 positive control. Exposure of cells to 12.5%-GBF media resulted in marked ROS production and
222 membrane permeability, which no thiol treatment alleviated.

223 *Dose-dependent toxicity of GBF is a function of growth temperature*

224 To evaluate the effects of GBF dosage on PCC 7002 physiology, we measured growth
225 rates in GBF concentrations ranging from 6.25%-12.5% (v/v) as a function of temperature (27°C
226 vs 37°C) and light intensity (100 µmol m⁻² s⁻¹ vs 200 µmol m⁻² s⁻¹) (Table 3). Medium A⁺
227 served as a control. Higher temperatures depressed growth rates in GBF-based media. At 37°C,

228 growth rates with 6.25% GBF at both $100 \mu\text{mol m}^{-2} \text{s}^{-1}$ and $200 \mu\text{mol m}^{-2} \text{s}^{-1}$ were most
229 comparable to Medium A⁺. Higher GBF concentrations had a more extreme effect on growth
230 rates. However, this dose dependent effect of GBF on growth rate was abolished when the
231 cultivation temperature was lowered to 27°C. At $200 \mu\text{mol m}^{-2} \text{s}^{-1}$ and 27°C, GBF cultures grew
232 twice as slowly as the control and there was no significant difference between the tested GBF
233 concentrations. Under $100 \mu\text{mol m}^{-2} \text{s}^{-1}$ and 27°C, growth rates were comparable across media
234 conditions. Thus, successful cultivation using the more concentrated GBF media required
235 adjusting both the light and temperature regimes.

236 Photobleaching is a common symptom of oxidative stress in photosynthetic organisms
237 and is caused by the accumulation of ROS (43). To investigate the effects of GBF media on the
238 photosynthetic pigmentation, we also performed whole cell absorbance scans at two different
239 temperatures (27°C vs 37°C). Light intensity was held constant at $200 \mu\text{mol m}^{-2} \text{s}^{-1}$. High GBF
240 concentrations yielded enhanced chlorophyll, phycobilisome, and carotenoid degradation at 37°C
241 (Figure 4a). At 27°C, photosynthetic pigments maintained intact relative to the control,
242 regardless of GBF concentration, implying less ROS production at this temperature (Figure 4b).

243 We wondered whether the observed toxicity was imposed on cells early or late during the
244 72-hour cultivation period. To track the dynamics of GBF induced toxicity, we employed
245 forward scatter flow cytometry using SYTO 59 as a counterstain to identify cells, which were
246 subsequently visualized for membrane integrity using Sytox Green. Two distinct phases were
247 identified upon exposure to GBF, which we interpreted as initial and chronic toxicity (Figure 4).
248 Initial toxicity was defined as the change in Sytox Green positive events for samples analyzed
249 during exponential growth, while chronic toxicity accounted for the change in Sytox Green
250 events during linear growth. As was the case for 72-hour based growth rate, a relationship

251 between both initial and chronic toxicity and increasing GBF concentrations was found at 37°C
252 (Figure 5a). While we still detected considerable initial toxicity with GBF exposure at 27°C,
253 there was less of an effect of dosage on chronic toxicity (Figure 5b). Altogether, this suggested
254 that there was a temperature and cell-concentration dependent adaptation that ameliorated the
255 susceptibility of cultures to GBF induced toxicity.

256 *Exposure to GBF retards oxygen evolution*

257 To better delineate the cause of initial toxicity associated with high GBF concentrations,
258 we measured maximal oxygen evolution rates for strains briefly exposed to GBF media while
259 increasing the light intensity. Measurements of photosynthetic oxygen evolution would allow for
260 an indirect assessment of PSII activity and electron transfer. Cultures were grown to early linear
261 phase in Medium A⁺ or GBF media, washed, and resuspended in the appropriate media.
262 Resuspension media was saturated with HCO₃⁻ (10 mM) in order to prevent inorganic carbon
263 limitation. As expected, cells grown and assayed in Medium A⁺ at 37°C showed a clear increase
264 in O₂ evolution rate as the light intensity approached saturation at 2700 μmol m⁻² s⁻¹, reaching a
265 maximal rate of 240 ± 8 μmol O₂ (mg Chl a)⁻¹ h⁻¹ (Figure 6a). Cells grown in Medium A⁺ at
266 37°C but assayed in 12.5% GBF had diminished O₂ evolution rates at all light intensities,
267 plateauing with a rate of 79 ± 6 μmol O₂ (mg Chl a)⁻¹ h⁻¹ at an intensity of 270 μmol m⁻² s⁻¹
268 (Figure 6a). Thus, exposure to GBF under these conditions immediately caused a decrease in O₂
269 production.

270 Next, we examined the effect of temperature in a similar experiment. Assays carried out
271 in Medium A⁺ after growth in Medium A⁺ at 27°C showed much higher maximal O₂ evolution
272 rates at all tested light intensities than with cells grown at 37°C (Figure 6b), peaking at a rate 556
273 ± 102 μmol O₂ (mg Chl a)⁻¹ h⁻¹). This was expected because elevated O₂ evolution rates in low

274 temperature grown cells have been previously reported and were attributed to a substantial
275 change in photosystem stoichiometry (44). The O₂ evolution rates of cells grown in Medium A⁺
276 at 27°C and then resuspended in 12.5% GBF stayed relatively constant at all of the tested
277 intensities and were roughly 5-fold lower than in controls, with a maximal rate of 109 ± 22 μmol
278 O₂ (mg Chl a)⁻¹ h⁻¹ at an intensity of 75 μmol m⁻² s⁻¹. We compared the above rates to those
279 from cultures grown in 12.5% GBF at 27°C to test if adaptation to GBF was met with changes in
280 photosynthetic activity. At tested light intensities, O₂ evolution rates with 27°C GBF-adapted
281 cultures were not statistically different than with unadapted cultures. Finally, we conducted the
282 inverse experiment, using cultures grown in GBF media at 27°C but assayed in Medium A⁺
283 under saturating light. Interestingly, they displayed the highest evolution rate of any tested
284 condition, at 944 ± 96 μmol O₂ (mg Chl a)⁻¹ h⁻¹ (Figure 6b). This suggested that there is a period
285 of dynamic photosynthetic adaptation to overcome the stress of GBF, and that when the stress is
286 alleviated the cells have an enhanced capacity for photosynthetic activity.

287

288 *Acclimation to GBF changes lipid content and composition*

289 Based on the results described above, we hypothesized that the temperature dependent
290 photosynthetic adaptation is related to changes in thylakoid membrane content and composition.
291 We extracted total fatty acids of cultures grown at 27°C for 72 hours in 12.5% GBF or Medium
292 A⁺, and analyzed the content after derivatization. We could detect and resolve all major saturated
293 and unsaturated fatty acid species (Table 4). Cultures grown in GBF had greater totals of assayed
294 fatty acid species (27 ± 7 mg FAME gDCW⁻¹) when compared to cells grown in Medium A⁺ (15
295 ± 1 mg FAME gDCW⁻¹) (Table 4). The most abundant fatty acid in all samples was 16:0 (42-
296 45% of the total fatty acids). C18:2 Δ^{9,12} fatty acids comprised a significant fraction of Medium

297 A⁺ grown cultures with 22% of the total fatty acid species. However, in GBF-grown cells the
298 amount of C18:2 Δ^{9,12} fatty acids was only 15%, while C18:3 Δ^{9,12,15} fatty acids were twice
299 as high in GBF grown cells (16%) than in Medium A⁺ grown cells (9%) (Table 4). This suggests
300 that cells were altering their membrane composition when grown in GBF, as compared to
301 standard growth in Medium A⁺.

302

303 **DISCUSSION**

304 The amount and distribution of arable land and potable water are projected to change
305 over the next several decades due to climate change, while the rise in global population and
306 standard of living are expected to increase demands (45). Integration of microalgal cultivation
307 with industrial and municipal wastewater treatment circumvents many of the resource concerns
308 raised over biofuel production (2), while simultaneously removing additional nutrients and
309 pollutants present in the wastewater (46). However, under standard environmental conditions we
310 were unable to obtain robust growth of PCC 7002 using a diluted municipal side stream as a
311 nutrient source. We hypothesized that this effect may be due to the presence of DOM, which has
312 been demonstrated to cause a decrease in photosynthetic performance in various strains of
313 cyanobacteria (47–49). We investigated the effects of light intensity and temperature on the
314 physiology of digestate grown cultures, in an effort to find conditions conducive to biomass
315 generation and better understand the mechanisms of DOM toxicity.

316 We found that cultivation temperature was an important factor that allowed for the
317 growth of PCC 7002 under high GBF concentrations. Numerous physiological processes are
318 altered at low temperatures (50). Notably, the fatty acyl chains in the both the cytoplasmic and
319 thylakoid membrane undergo a transition from a fluid to nonfluid state (51). The immediate

320 cessation of oxygen evolution (Figure 6) and high rates of initial toxicity (Figure 5) upon GBF
321 exposure with cells cultivated at tested temperatures suggests that the toxic compound rapidly
322 crosses bacterial membranes. We propose that due to the decreased fluidity of the outer
323 membrane at 27°C relative to 37°C, accessibility of humic and fulvic acids to the hydrophobic
324 domains in the phospholipid bilayer is decreased, lessening the intracellular transport of the
325 toxic compound(s) and initial and chronic toxicity.

326 Upon a shift to a lower temperature, cyanobacteria also alter the expression of
327 desaturases to increase the unsaturated fatty acid content and maintain optimal membrane
328 function (52). Optimal fluidity of thylakoid membranes is a critical factor in photosynthetic
329 electron transport, due to the mobility of co-utilized redox components to both photosynthetic
330 and respiratory complexes to ensure ideal electron flow (53, 54). It has been shown that
331 temperature influences the kinetics governing the redox state of plastoquinone (PQ) through
332 alterations in thylakoid membrane composition and fluidity (55). We believe that this
333 temperature dependent alteration of the thylakoid membrane to circumvent GBF induced
334 changes in the redox state is also an important component of the adaptive response, given the
335 increase in unsaturated fatty acids observed during cultivation in GBF-based media (Table 4).

336 We propose that the herbicidal effect of GBF is partially due to the electron scavenging
337 properties of phenolic moieties within in the DOM, given the symptoms of chlorophyll-
338 bleaching as shown in Figure 3 and pronounced ROS production as evidenced by Figure 2 (56).
339 These phenolic moieties are likely a component of the “soluble microbial products” found in our
340 EEM scans (Figure 2). At low concentrations, phenolic photosynthetic electron transfer
341 inhibitors such as 2,5-Dibromo-3-methyl-6-isopropyl-p-benzoquinone (DBMIB), alter the redox
342 potential of the PQ pool of PSII by blocking forward electron transfer to the cytochrome b_6/f

343 complex (57). DBMIB treatment has also been shown to substantially decrease inner
344 mitochondrial membrane fluidity (58). This strong reduction of the PQ pool by DBMIB induces
345 the phycobilisomes to physically move from PSII to PSI in a transition known as “state 2”,
346 thereby decreasing the ratio of reducing power to proton-motive force generated by
347 photosynthesis (59). Marine *Synechococcus*, including PCC 7002, have also been shown to
348 transition to state 2 upon shifts to lower temperature (60). Chronic exposure to phenolic
349 herbicides eventually leads to radical-catalyzed back reactions that trigger the formation of ROS
350 that facilitate complex destruction and cell death (43, 61–63). Some phenolic herbicides may
351 also act as arylating agents, causing covalent binding to macromolecules via Michael addition
352 and a depletion of thiol pools (64). The inability of the reducing agents we tested to maintain
353 membrane integrity suggests that GBF-induced cytotoxicity is likely caused by redox cycling,
354 and not arylation. Future efforts to increase tolerance to these toxicants might include disruption
355 of the inhibitor binding sites (65, 66) or optimizing membrane fluidity (67).

356 **CONCLUSIONS**

357 Under standard cultivation conditions of 37°C with the cyanobacteria *Synechococcus* sp.
358 strain PCC 7002, there was a dose-dependent relationship between liquid anaerobic digestate
359 concentration and toxicity. This was met with ROS production and photopigment degradation.
360 Digestate contained constituents of dissolved organic matter that were likely affecting
361 photosynthetic electron transport. Decreasing the cultivation temperature to 27°C enabled robust
362 cultivation at high digestate concentrations, resulting in high biomass productivities. This
363 temperature dependent tolerance may be due to changes in membrane fluidity. Our study
364 highlights the contributions of dissolved organic matter to photosynthetic growth and physiology
365 in wastewater based media, as well as a potential mechanism for tolerance in low temperatures.

366 **ACKNOWLEDGEMENTS**

367 This work was funded by the US National Science Foundation (EFRI-1240268). TCK is
368 the recipient of a National Institutes of Health (NIH) Biotechnology Training Fellowship
369 (NIGMS-5 T32 GM08349) and a fellowship from the UW-Madison College of Engineering's
370 Graduate Engineering Research Scholars (GERS) program. The authors are grateful to Richard
371 Mikel, Matthew Dysthe, and Derek Jacobs for help with routine sampling.

REFERENCES

1. Oliver JWK, Atsumi S. 2014. Metabolic design for cyanobacterial chemical synthesis. *Photosynth Res* 120:249–61.
2. Pate R, Klise G, Wu B. 2011. Resource demand implications for US algae biofuels
5 production scale-up. *Appl Energy* 88:3377–3388.
3. Clarens AF, Resurreccion EP, White M a, Colosi LM. 2010. Environmental life cycle comparison of algae to other bioenergy feedstocks. *Environ Sci Technol* 44:1813–9.
4. Posadas E, García-Encina PA, Domínguez A, Díaz I, Becares E, Blanco S, Muñoz R. 2014. Enclosed tubular and open algal-bacterial biofilm photobioreactors for carbon and
10 nutrient removal from domestic wastewater. *Ecol Eng* 67:156–164.
5. Sturm BSM, Lamer SL. 2011. An energy evaluation of coupling nutrient removal from wastewater with algal biomass production. *Appl Energy* 88:3499–3506.
6. Hoffmann JP. 1998. Wastewater Treatment with Suspended and Nonsuspended Algae. *J Phycol* 34:757–763.
- 15 7. de la Noüe J, Laliberté G, Proulx D. 1992. Algae and waste water. *J Appl Phycol* 4:247–254.
8. Olguín EJ. 2012. Dual purpose microalgae–bacteria-based systems that treat wastewater and produce biodiesel and chemical products within a Biorefinery. *Biotechnol Adv* 30:1031–1046.
- 20 9. Wang L, Min M, Li Y, Chen P, Chen Y, Liu Y, Wang Y, Ruan R. 2010. Cultivation of green algae *Chlorella* sp. in different wastewaters from municipal wastewater treatment plant. *Appl Biochem Biotechnol* 162:1174–86.
10. Peccia J, Haznedaroglu B, Gutierrez J, Zimmerman JB. 2013. Nitrogen supply is an

- important driver of sustainable microalgae biofuel production. *Trends Biotechnol* 31:134–8.
11. Rawat I, Ranjith Kumar R, Mutanda T, Bux F. 2011. Dual role of microalgae: Phycoremediation of domestic wastewater and biomass production for sustainable biofuels production. *Appl Energy* 88:3411–3424.
12. Pflugmacher S, Spangenberg M, Steinberg CEW. 1999. Dissolved organic matter (DOM) and effects on the aquatic macrophyte *Ceratophyllum demersum* in relation to photosynthesis, pigment pattern and activity of detoxication enzymes. *J Appl Bot* 73:184–190.
13. Zsolnay Á. 2003. Dissolved organic matter: Artefacts, definitions, and functions, p. 187–209. *In* Geoderma.
14. Imai A, Fukushima T, Matsushige K, Kim Y-H, Choi K. 2002. Characterization of dissolved organic matter in effluents from wastewater treatment plants. *Water Res* 36:859–870.
15. Akhlar A, Torrijos M, Battimelli A, Carrère H. 2016. Comprehensive characterization of the liquid fraction of digestates from full-scale anaerobic co-digestion. *Waste Manag.*
16. Vigneault B, Percot A, Lafleur M, Campbell PGC. 2000. Permeability changes in model and phytoplankton membranes in the presence of aquatic humic substances. *Environ Sci Technol* 34:3907–3913.
17. Ojwang' LM, Cook RL. 2013. Environmental Conditions That Influence the Ability of Humic Acids to Induce Permeability in Model Biomembranes. *Environ Sci Technol* 47:8280–8287.
18. Chiou CT, Malcolm RL, Brinton TI, Kile DE. 1986. Water solubility enhancement of

some organic pollutants and pesticides by dissolved humic and fulvic acids. *Environ Sci Technol*; (United States) 20.

19. Zhang D, Yan S, Song W. 2014. Photochemically Induced Formation of Reactive Oxygen Species (ROS) from Effluents Organic Matter. *Environ Sci Technol*.
- 5 20. Lee E, Glover CM, Rosario-Ortiz FL. 2013. Photochemical formation of hydroxyl radical from effluent organic matter: Role of composition. *Environ Sci Technol* 47:12073–12080.
21. Laue P, Bährs H, Chakrabarti S, Steinberg CEW. 2014. Natural xenobiotics to prevent cyanobacterial and algal growth in freshwater: Contrasting efficacy of tannic acid, gallic acid, and gramine. *Chemosphere* 104:212–220.
- 10 22. Keren N, Krieger-Liszkay A. 2011. Photoinhibition: molecular mechanisms and physiological significance. *Physiol Plant* 142:1–5.
23. Nagano T, Kojima K, Hisabori T, Hayashi H, Morita EH, Kanamori T, Miyagi T, Ueda T, Nishiyama Y. 2012. Elongation factor G is a critical target during oxidative damage to the translation system of *Escherichia coli*. *J Biol Chem* 287:28697–704.
- 15 24. Foyer CH, Neukermans J, Queval G, Noctor G, Harbinson J. 2012. Photosynthetic control of electron transport and the regulation of gene expression. *J Exp Bot* 63:1637–61.
25. Voss I, Sunil B, Scheibe R, Raghavendra AS. 2013. Emerging concept for the role of photorespiration as an important part of abiotic stress response. *Plant Biol (Stuttg)* 15:713–22.
- 20 26. Ruffing AM. 2011. Engineered cyanobacteria: Teaching an old bug new tricks. *bioe* 2:136–149.
27. Xu Y, Alvey RM, Byrne PO, Graham JE, Shen G, Bryant DA. 2011. Expression of genes in cyanobacteria: adaptation of endogenous plasmids as platforms for high-level gene

- expression in *Synechococcus* sp. PCC 7002. *Methods Mol Biol* 684:273–93.
28. Stevens SE, Patterson COP, Myers J. 1973. The Production of Hydrogen Peroxide by Blue-Green Algae: A Survey. *J Phycol* 9:427–430.
29. Sakamoto T, Bryant DA. 2001. Requirement of Nickel as an Essential Micronutrient for the Utilization of Urea in the Marine Cyanobacterium *Synechococcus* sp. PCC 7002. *Microbes Environ* 16:177–184.
30. Flowers JJ, Cadkin TA, McMahon KD. 2013. Seasonal bacterial community dynamics in a full-scale enhanced biological phosphorus removal plant. *Water Res* 47:7019–7031.
31. He S, McMahon KD. 2011. “*Candidatus Accumulibacter*” gene expression in response to dynamic EBPR conditions. *ISME J* 5:329–40.
32. Eaton AD, Franson MAH. 2005. *Standard Methods for the Examination of Water & Wastewater*, 21sted. American Public Health Association.
33. Lennen RM, Braden DJ, West RA, Dumesic JA, Pfleger BF. 2010. A process for microbial hydrocarbon synthesis: Overproduction of fatty acids in *Escherichia coli* and catalytic conversion to alkanes. *Biotechnol Bioeng* 106:193–202.
34. Sakamoto T, Bryant D a. 2002. Synergistic effect of high-light and low temperature on cell growth of the Delta12 fatty acid desaturase mutant in *Synechococcus* sp. PCC 7002. *Photosynth Res* 72:231–42.
35. Miyashita H, Adachi K, Kurano N, Ikemot H, Chihara M, Miyach S. 1997. Pigment composition of a novel oxygenic photosynthetic prokaryote containing chlorophyll d as the major chlorophyll. *Plant cell Physiol* 38:274–281.
36. Porra RJ, Thompson WA, Kriedemann PE. 1989. Determination of accurate extinction coefficients and simultaneous equations for assaying chlorophylls a and b extracted with

- four different solvents: verification of the concentration of chlorophyll standards by atomic absorption spectroscopy. *Biochim Biophys Acta (BBA)-Bioenergetics* 975:384–394.
37. Chen W, Westerhoff P, Leenheer JA, Booksh K. 2003. Fluorescence Excitation-Emission Matrix Regional Integration to Quantify Spectra for Dissolved Organic Matter. *Environ Sci Technol* 37:5701–5710.
38. Lehmann J, Kleber M. 2015. The contentious nature of soil organic matter. *Nature* 1–9.
39. Peña-méndez ME, Havel J, Patočka J. 2005. Humic substances – compounds of still unknown structure□: applications in agriculture , industry , environment , and
10 biomedicine. *J Appl Biomed* 3:13–24.
40. Cowgill RW. 1963. Fluorescence and the structure of proteins. I. Effects of substituents on the fluorescence of indole and phenol compounds. *Arch Biochem Biophys* 100:36–44.
41. Dignac MF, Ginestet P, Rybacki D, Bruchet A, Urbain V, Scribe P. 2000. Fate of wastewater organic pollution during activated sludge treatment: Nature of residual organic
15 matter. *Water Res* 34:4185–4194.
42. Samuni Y, Goldstein S, Dean OM, Berk M. 2013. The chemistry and biological activities of N-acetylcysteine. *Biochem Biophys* 1830:4117–4129.
43. Latifi A, Ruiz M, Zhang C-C. 2009. Oxidative stress in cyanobacteria. *FEMS Microbiol Rev* 33:258–78.
- 20 44. Sakamoto T, Bryant D a. 1998. Growth at low temperature causes nitrogen limitation in the cyanobacterium *Synechococcus* sp. PCC 7002. *Arch Microbiol* 169:10–9.
45. Parry ML, Rosenzweig C, Iglesias A, Livermore M, Fischer G. 2004. Effects of climate change on global food production under SRES emissions and socio-economic scenarios.

Glob Environ Chang 14:53–67.

46. Wang Y, Ho SH, Cheng CL, Guo WQ, Nagarajan D, Ren NQ, Lee DJ, Chang JS. 2016. Perspectives on the feasibility of using microalgae for industrial wastewater treatment. *Bioresour Technol* 222:485–497.
- 5 47. Sun B, Tanji Y, Unno H. 2006. Extinction of cells of cyanobacterium *Anabaena circinalis* in the presence of humic acid under illumination. *Appl Microbiol Biotechnol* 72:823–828.
48. Shao J, Wu Z, Yu G, Peng X, Li R. 2009. Allelopathic mechanism of pyrogallol to *Microcystis aeruginosa* PCC7806 (Cyanobacteria): From views of gene expression and antioxidant system. *Chemosphere* 75:924–928.
- 10 49. Gjessing ET, Alberts J., Bruchet A, Egeberg PK, Lydersen E, McGown LB, Mobed JJ, Münster U, Pempkowiak J, Perdue M, Ratnawerra H, Rybacki D, Takacs M, Abbt-Braun G. 1998. Multi-method characterisation of natural organic matter isolated from water: characterisation of reverse osmosis-isolates from water of two semi-identical dystrophic lakes basins in Norway. *Water Res* 32:3108–3124.
- 15 50. Morgan-Kiss RM, Priscu JC, Pocock T, Gudynaite-Savitch L, Huner NPA. 2006. Adaptation and Acclimation of Photosynthetic Microorganisms to Permanently Cold Environments. *Microbiol Mol Biol Rev* 70:222–252.
51. De Mendoza D. 2014. Temperature Sensing by Membranes. *Annu Rev Microbiol* 68:101–16.
- 20 52. Singh SC, Sinha RP, Häder D. 2002. Role of Lipids and Fatty Acids in Stress Tolerance in Cyanobacteria. *Acta Protozool* 41:297–308.
53. Mullineaux CW. 2014. Electron transport and light-harvesting switches in cyanobacteria. *Front Plant Sci* 5:1–6.

54. Liu L-N. 2015. Distribution and dynamics of electron transport complexes in cyanobacterial thylakoid membranes. *Biochim Biophys Acta - Bioenerg.*
55. Klementiev KE, Tsoraev G V, Tyutyayev E V, Zorina AA, Feduraev P V, Allakhverdiev SI, Paschenko VZ. 2017. Membrane fluidity controls redox-regulated cold stress responses in cyanobacteria. *Photosynth Res* 0:0.
56. Pallett KE, Dodge AD. 1980. Studies into the Action of Some Photosynthetic Inhibitor Herbicides. *J Exp Bot* 31:1051–1066.
57. Schoepp B, Brugna M, Riedel A, Nitschke W, Kramer DM. 1999. The Qo-site inhibitor DBMIB favours the proximal position of the chloroplast Rieske protein and induces a pK-shift of the redox-linked proton. *FEBS Lett* 450:245–250.
58. Siedow JN, Huber SC, Moreland DE. 1979. Effects of dibromothymoquinone on mung bean mitochondrial electron transfer and membrane fluidity. *BBA - Bioenerg* 547:282–295.
59. Mao H Bin, Li GF, Ruan X, Wu QY, Gong YD, Zhang XF, Zhao NM. 2002. The redox state of plastoquinone pool regulates state transitions via cytochrome b6f complex in *Synechocystis* sp. PCC 6803. *FEBS Lett* 519:82–86.
60. Mackey KRM, Paytan A, Caldeira K, Grossman AR, Moran D, McIlvin M, Saito MA. 2013. Effect of temperature on photosynthesis and growth in marine *Synechococcus* spp. *Plant Physiol* 163:815–29.
61. Krieger-Liszkay A, Fufezan C, Trebst A. 2008. Singlet oxygen production in photosystem II and related protection mechanism. *Photosynth Res* 98:551–564.
62. Idedan I, Tomo T, Noguchi T. 2011. Herbicide effect on the photodamage process of photosystem II: Fourier transform infrared study. *Biochim Biophys Acta - Bioenerg*

1807:1214–1220.

63. Nishiyama Y, Allakhverdiev SI, Murata N. 2011. Protein synthesis is the primary target of reactive oxygen species in the photoinhibition of photosystem II. *Physiol Plant* 142:35–46.
64. Wang X, Thomas B, Sachdeva R, Arterburn L, Frye L, Hatcher PG, Cornwell DG, Ma J. 2006. Mechanism of arylating quinone toxicity involving Michael adduct formation and induction of endoplasmic reticulum stress. *Proc Natl Acad Sci U S A* 103:3604–9.
65. Ajlani G, Kirilovsky D, Picaud M, Astier C. 1989. Molecular analysis of *psbA* mutations responsible for various herbicide resistance phenotypes in *Synechocystis* 6714. *Plant Mol Biol* 13:469–79.
- 10 66. Lee TX, Metzger SU, Cho YS, Whitmarsh J, Kallas T. 2001. Modification of inhibitor binding sites in the cytochrome *bf* complex by directed mutagenesis of cytochrome *b6* in *Synechococcus* sp. PCC 7002. *Biochim Biophys Acta - Bioenerg* 1504:235–247.
67. Gombos Z, Wada H, Murata N. 1994. The recovery of photosynthesis from low-temperature photoinhibition is accelerated by the unsaturation of membrane lipids: a mechanism of chilling tolerance. *Proc Natl Acad Sci U S A* 91:8787–91.
- 15

FIGURE LEGENDS

Figure 1. Flow diagram and nutrient streams obtained from the Nine Springs Wastewater Treatment Plant (Dane County, Wisconsin, USA). Stars indicate sampling points.

5

Figure 2. Excitation Emission Matrix of wastewater medias. Fluorescence values were normalized to 1 ppm of quinine sulfate in 0.1 N H₂SO₄ at Ex/Em = 350/450 nm.

Figure 3. Reactive oxygen species and membrane integrity assay. Cells were grown to early linear phase in Medium A⁺ or 12.5% GBF with the appropriate treatment under continuous illumination (200 μE m⁻² s⁻¹) with 1 % CO₂ at 37°C. Fluorescence values were normalized to OD₇₃₀. The values represent the mean ± SD of biological triplicates.

Figure 4. Absorption spectra of GBF exposed strains as a function of temperature. Cultures were grown in Medium A⁺, 6.25 %, or 12.5 % (v/v) GBF media under continuous illumination (200 μE m⁻² s⁻¹) with 1 % CO₂ at 37°C (A) or 27°C (B) for 72 hours. The spectra were recorded in dilute cell suspensions and normalized to an OD₇₃₀. The peak at 637 nm is due to phycobilisomes, the peak at 683 nm is due to chlorophyll a, and the peak at 438 nm is due to carotenoids.

20

Figure 5. Initial and chronic toxicity of cultures grown in Medium A⁺, 6.25 %, 9.9 %, or 12.5 % (v/v) GBF media under continuous illumination (200 μE m⁻² s⁻¹) with 1 % CO₂ at 37°C (A) or

27°C (B) for 72 hours. Initial toxicity was defined as the change in Sytox Green positive events for samples analyzed during exponential growth. Chronic toxicity accounted for the change in Sytox Green events during linear growth. A measure of < 0 chronic toxicity means that the samples recovered following a period of initial toxicity.

5

Figure 6. Rates of oxygen evolution as a function of acclimation temperature and light intensity.

Cells were grown to early linear phase in Medium A⁺ or 12.5% GBF under continuous illumination ($200 \mu\text{E m}^{-2} \text{s}^{-1}$) with 1 % CO₂ at 37°C (A) or 27°C (B). Cells were pelleted, resuspended in Medium A⁺ or 12.5% GBF, and the rate of maximal oxygen evolution was measured with 10 mM HCO₃⁻ as an electron acceptor at increasing light intensities. The values represent the mean \pm SE of biological duplicates.

10

TABLES

Table 1. Nutrient composition of batch of 100% GBF used for subsequent experiments

Analyte	Concentration ^a (mg L ⁻¹) (±SD)
NH ₃ -N	1180 ± 135
NO ₃ -N	7.5 ± 0.04
SRP	78 ± 10
COD	735 ± 4
TSS	467 ± 123
VSS	18 ± 2
TS	2350 ± 36
TS (Glass Fiber Filtered)	2030 ± 42
TS (0.45 um membrane filtered)	2000 ± 151

^aValues shown represent the mean ± standard deviation (SD) of at least three technical replicates.

Table 2. Characteristics of GBF and secondary effluent over the 6 month experimental period.

Source	Analyte	Concentration ^a (mg L ⁻¹) (±COV)
GBF	NH ₃ -N	920 ± 22%
	NO ₃ -N	3.9 ± 43%
	SRP	54 ± 27%
	NH ₃ -N	n.d.
Secondary Effluent	NO ₃ -N	19.3 ± 6.6%
	SRP	n.d.

^aValues shown represent the mean ± coefficient of variation (COV) of at least three technical replicates.

Table 3. Growth Rates with varying Temperature and Light Intensity

Media	Light Intensity ($\mu\text{E m}^{-2} \text{s}^{-1}$)	Temperature ($^{\circ}\text{C}$)	Growth Rate ($\pm\text{SD}$) (OD day^{-1})
A ⁺	200	37	0.66 \pm 0.04
6.25% GBF	200	37	0.58 \pm 0.05
12.5% GBF	200	37	0.05 \pm 0.01
A ⁺	100	37	0.28 \pm 0.01
6.25% GBF	100	37	0.24 \pm 0.01
9.9% GBF	100	37	0.11 \pm 0.02
12.5% GBF	100	37	0.02 \pm 0.00
A ⁺	200	27	0.73 \pm 0.08
6.25% GBF	200	27	0.32 \pm 0.03
9.9% GBF	200	27	0.42 \pm 0.06
12.5% GBF	200	27	0.28 \pm 0.04
A ⁺	100	27	0.25 \pm 0.01
6.25% GBF	100	27	0.26 \pm 0.02
9.9% GBF	100	27	0.24 \pm 0.01
12.5% GBF	100	27	0.26 \pm 0.02

^a Linear growth rates of cultures grown in Medium A⁺ or GBF with the appropriate treatment under continuous illumination ($200 \mu\text{E m}^{-2} \text{s}^{-1}$ or $100 \mu\text{E m}^{-2} \text{s}^{-1}$) with 1 % CO₂ at 37°C or 27°C.

5 The values represent the mean \pm SD of biological triplicates.

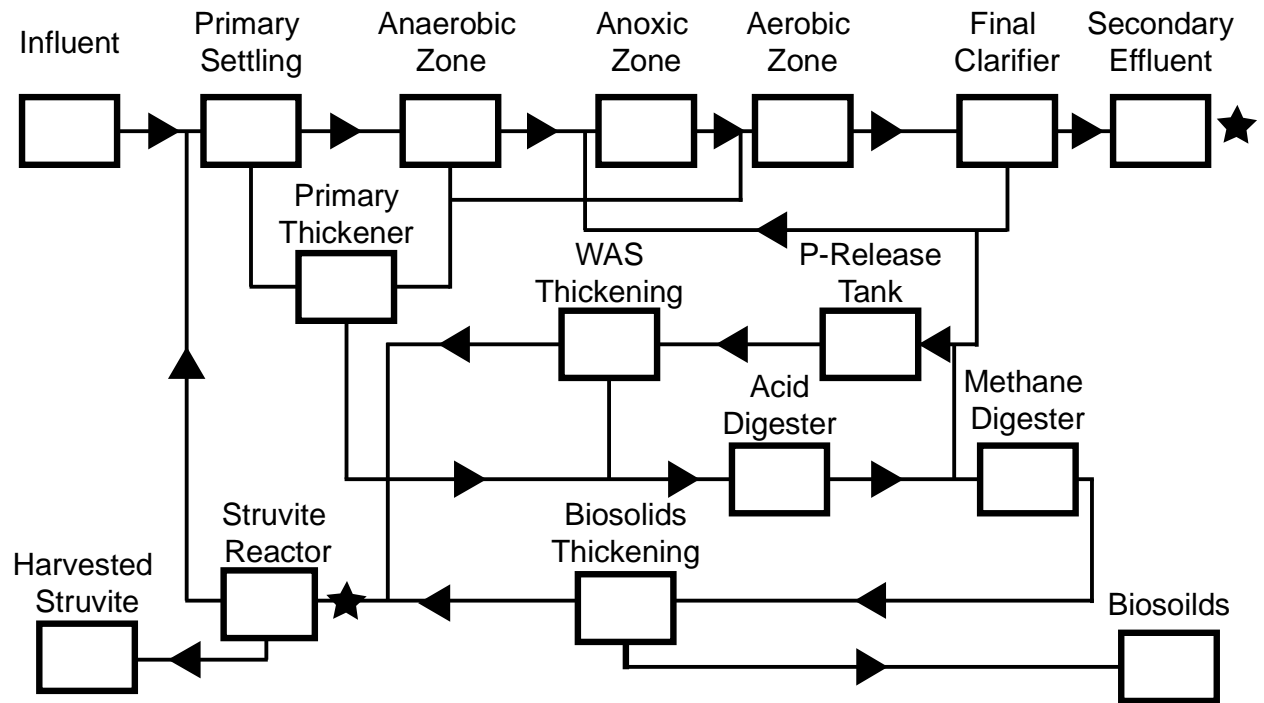
Table 4. Fatty acid content and composition of cultures grown in Medium A⁺ or 12.5% GBF media under continuous illumination (200 $\mu\text{E m}^{-2} \text{s}^{-1}$) at 27°C for 72 hours

Growth Conditions ¹		Fatty Acids Species					
		C16:0	C16:1 Δ 9	C18:0	C18:1 Δ 9	C18:2 Δ 9,12	C18:3 Δ 9,12,1
Medium A ⁺	mg FA gDCW ⁻¹	6.7 \pm 0.7	2.0 \pm 0.1	0.2 \pm 0.1	1.5 \pm 0.2	3.3 \pm 0.2	1.4 \pm 0.
	% FA	44 \pm 1	13 \pm 1	2 \pm 0	10 \pm 0	22 \pm 1	9 \pm 1
GBF	mg FA gDCW ⁻¹	11.6 \pm 3.1	3.5 \pm 0.8	1.3 \pm 0.3	2.2 \pm 0.7	3.9 \pm 0.8	4.4 \pm 1.
	% FA	43 \pm 0	13 \pm 0	5 \pm 0	8 \pm 0	15 \pm 1	16 \pm 1

¹Strains were grown in the Medium A⁺ or 12.5% GBF media under continuous illumination (200 $\mu\text{E m}^{-2} \text{s}^{-1}$) at 27°C for 72 hours. Fatty acids were extracted and derivatized as previously

5 described. The values represent the mean \pm SD of two independent experiments.

FIGURES



5

Figure 1. Flow diagram and nutrient streams obtained from the Nine Springs Wastewater Treatment Plant (Dane County, Wisconsin, USA). Stars indicate sampling points.

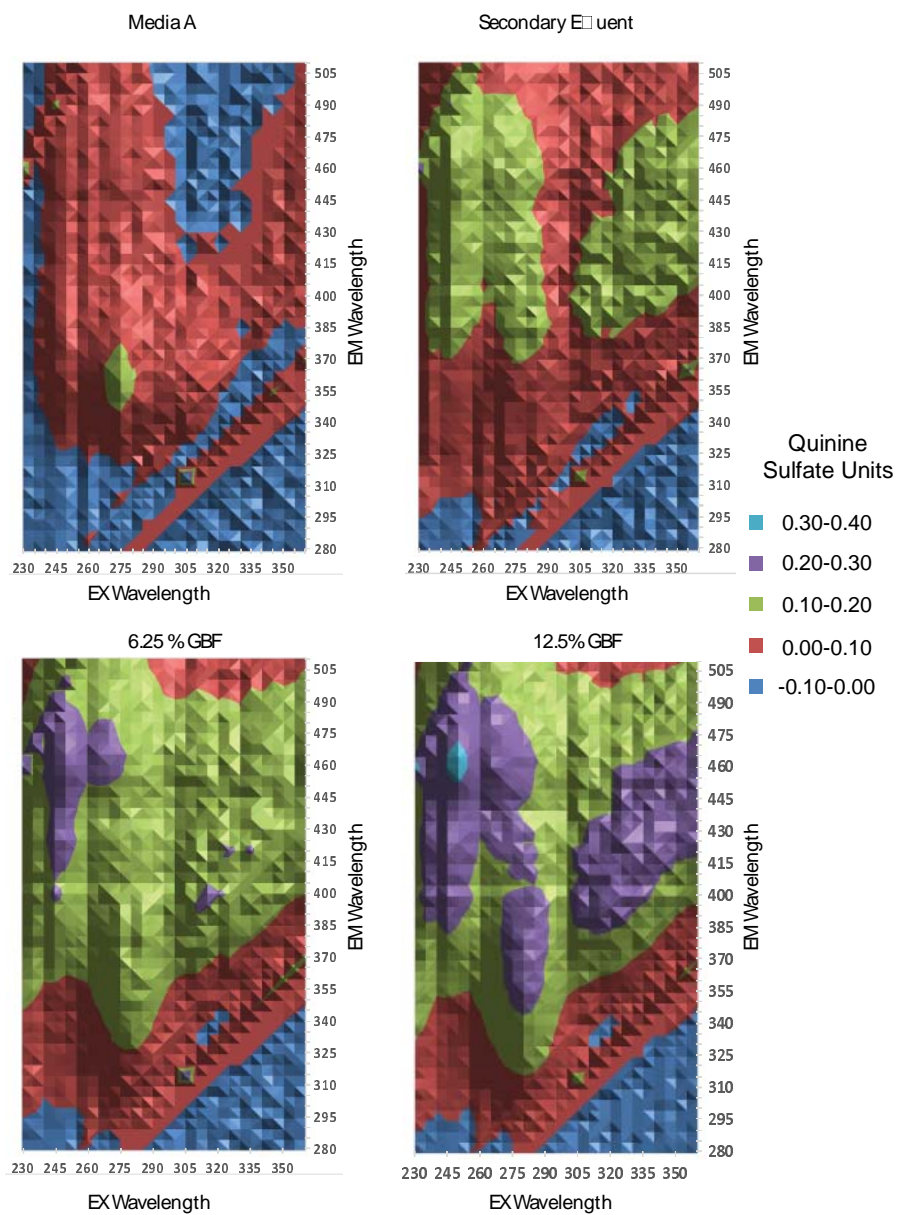


Figure 2. Excitation Emission Matrix of wastewater medias. Fluorescence values were normalized to 1 ppm of quinine sulfate in 0.1 N H₂SO₄ at Ex/Em = 350/450 nm.

ROS and Membrane Integrity

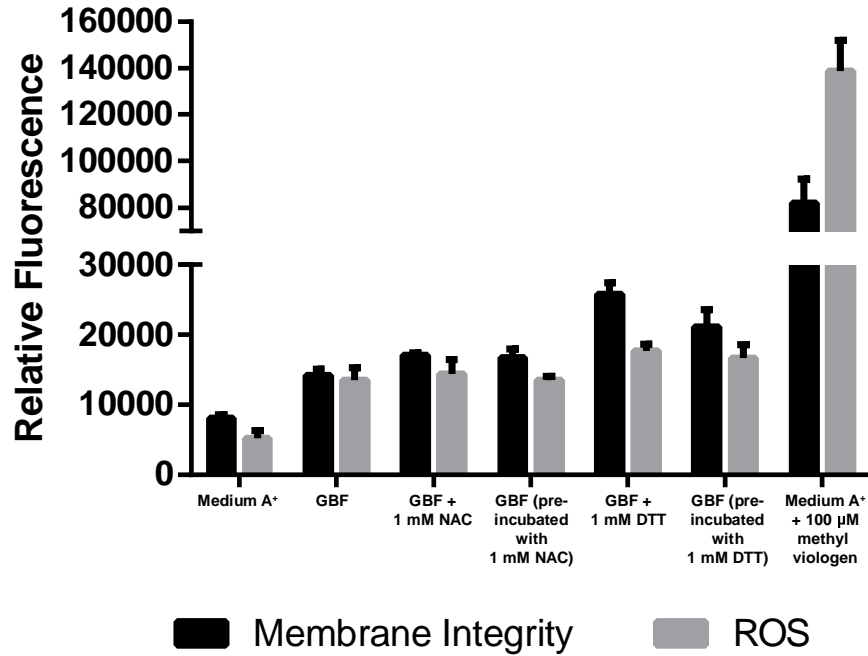


Figure 3. Reactive oxygen species and membrane integrity assay. Cells were grown to early linear phase in Medium A⁺ or 12.5% GBF with the appropriate treatment under continuous illumination ($200 \mu\text{E m}^{-2} \text{s}^{-1}$) with 1 % CO₂ at 37°C. Fluorescence values were normalized to 5 OD₇₃₀. The values represent the mean \pm SD of biological triplicates.

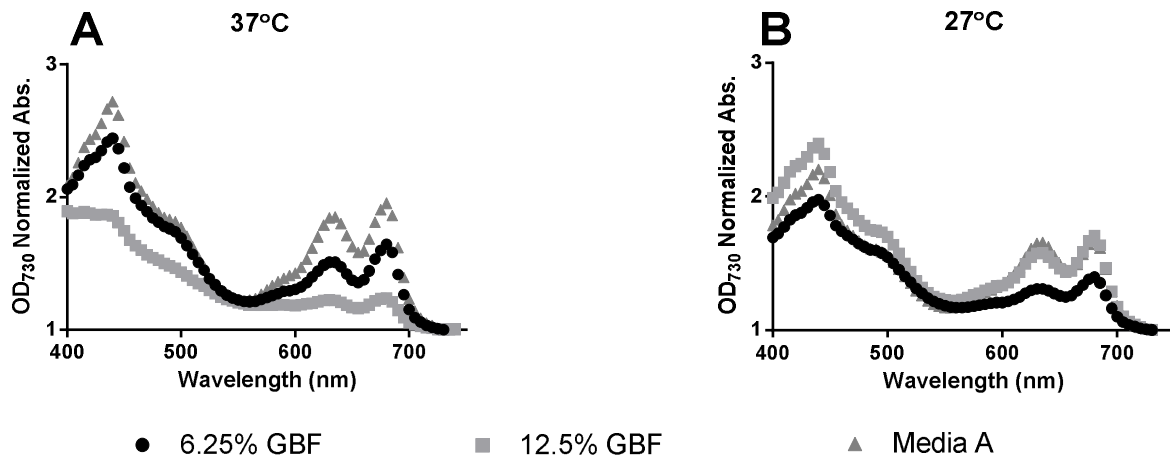


Figure 4. Absorption spectra of GBF exposed strains as a function of temperature. Cultures were grown in Medium A⁺, 6.25 %, or 12.5 % (v/v) GBF media under continuous illumination ($200 \mu\text{E m}^{-2} \text{s}^{-1}$) with 1 % CO₂ at 37°C (A) or 27°C (B) for 72 hours. The spectra were recorded in dilute cell suspensions and normalized to an OD₇₃₀. The peak at 637 nm is due to phycobilisomes, the peak at 683 nm is due to chlorophyll a, and the peak at 438 nm is due to carotenoids.

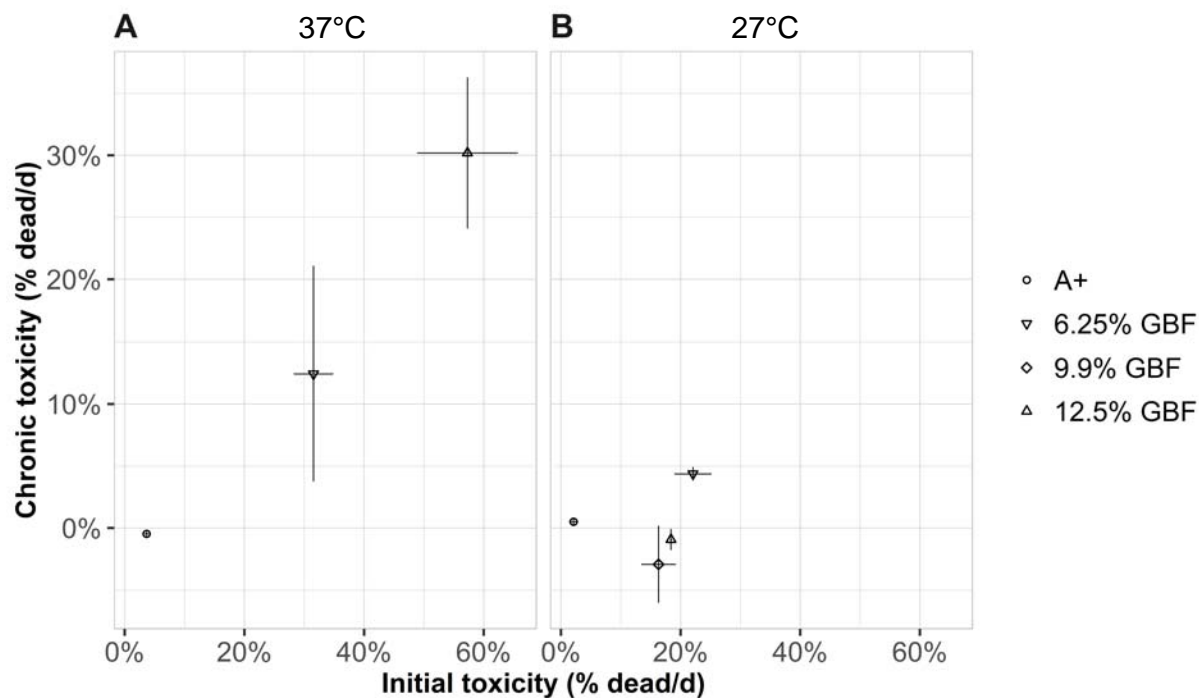


Figure 5. Initial and chronic toxicity of cultures grown in Medium A⁺, 6.25 %, 9.9 %, or 12.5 % (v/v) GBF media under continuous illumination ($200 \mu\text{E m}^{-2} \text{s}^{-1}$) with 1 % CO₂ at 37°C (A) or 27°C (B) for 72 hours. Initial toxicity was defined as the change in Sytox Green positive events for samples analyzed during exponential growth. Chronic toxicity accounted for the change in Sytox Green events during linear growth. A measure of < 0 chronic toxicity means that the samples recovered following a period of initial toxicity.

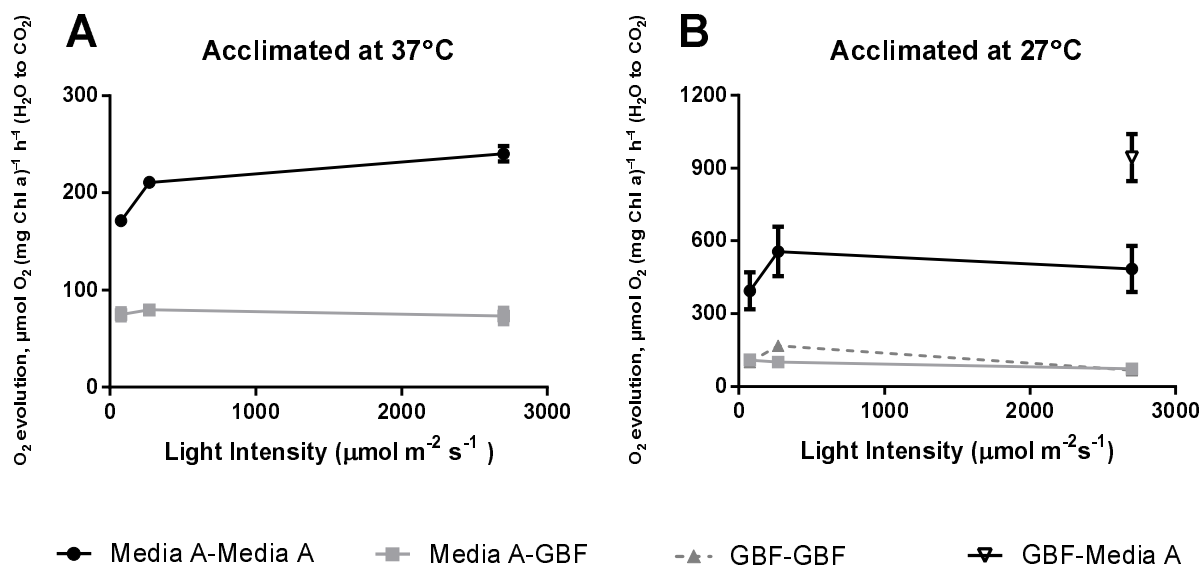


Figure 6. Rates of oxygen evolution as a function of acclimation temperature and light intensity.

Cells were grown to early linear phase in Medium A⁺ or 12.5% GBF under continuous illumination ($200 \mu\text{E m}^{-2} \text{s}^{-1}$) with 1 % CO₂ at 37°C (A) or 27°C (B). Cells were pelleted, resuspended in Medium A⁺ or 12.5% GBF, and the rate of maximal oxygen evolution was measured with 10 mM HCO₃⁻ as an electron acceptor at increasing light intensities. The values represent the mean \pm SE of biological duplicates.